Asociación Argentina
de Mecánica Computacional

Mecánica Computacional Vol XXIX, págs. 3347-3358 (artículo completo)
Eduardo Dvorkin, Marcela Goldschmit, Mario Storti (Eds.)
Buenos Aires, Argentina, 15-18 Noviembre 2010

INFLUENCE STUDY OF THE ENTRANCE CHANNEL IN A TWO-DIMENSIONAL BACKWARD-FACING STEP FLOW

Rogério Gonçalves dos Santos, Kéteri Poliane Moraes de Oliveira and José Ricardo Figueiredo

Faculdade de Engenharia Mecânica, Universidade Estadual de Campinas, Rua Mendeleyev, 200 - CEP 13083-860 - Cidade Universitária "Zeferino Vaz" Barão Geraldo - Campinas - SP, Brazil
figueiredo@fem.unicamp.br, http://www.fem.unicamp.br

Keywords: backward-facing step flow, Numerical Simulation, UNIFAES.

Abstract. The influence of the entrance channel in the numerical simulation of the classic two-dimensional backward-facing incompressible step flow was studied. Locations of detachment and reattachment, as well as velocity profile, were obtained as functions of Reynolds number. The Unified Finite Approach Exponential-type Scheme (UNIFAES) was employed in the discretization of the advective and viscous fluxes of the Navier-Stokes equations in primitive variables. The almost unknown semi-staggered mesh was used. The momentum equations are integrated explicitly after the solution of a Poisson pressure that enforces mass conservation. Richardson extrapolation is employed to estimate the correct solutions. As could be expected, using the entrance channel provided better agreement with experiments than not using it, particularly for producing a non-symmetric, decentralized flow profile at the step plane, instead of the assumed symmetric profile. Also, the size of first bubble is smaller, and the size of the second bubble is bigger.

1 INTRODUCTION

Backward-facing step flows represents a kind of problems with enormous importance in industrial applications. The detachment and reattachment points in the flow and its structure determine, for example, the local heat and mass transfer in a gas turbine. Understandably, the classic backward-facing incompressible step flow has been used extensively to test numerical methods. The importance of this test case motivated experimental investigation in laboratory models. The best known are Armaly et al. (1983) and Lee and Mateescu (1998) works, which was chosen here for being considered more reliable then Armaly et al.'s.

Anyway, the two-dimensional solutions obtained with the best numerical methods tend to closely approach the numerical results until Reynolds numbers about 700. For higher values, the distance between experiments and numerics tend to increase. One possible reason for such differences could be that most of the numerical results employ a rectangular domain, by which the flow emerging from the physical inlet slot is assumed to enter the domain at the step as a fully developed laminar flow with a parabolic velocity profile. However, a more careful modeling must consider the slot before the inlet. This paper compares the two alternatives, with and without the slot, and the experimental results by Lee and Mateescu (1998).

2 METHODOLOGY

The Unified Finite Approach Exponential-type Scheme (UNIFAES) was employed in the discretization of the advective and viscous fluxes of the Navier-Stokes equations in primitive variables. The almost unknown semi-staggered mesh was used. The momentum equations are integrated explicitly after the solution of a Poisson pressure that enforces mass conservation. Richardson extrapolation is employed to estimate the correct solutions.

2.1 Mesh

The present simulation uses the semi-staggered mesh structure, which combines vertex collocated velocity components and cell-centered pressure, as indicated in Fig. 1.

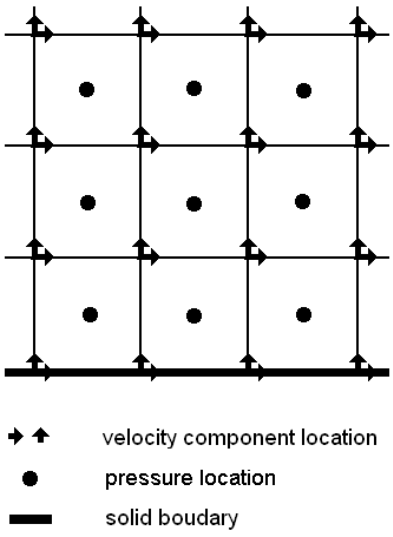

Figure 1: Semi-staggered mesh

This mesh, much less known then either the staggered mesh or the cell-center collocated mesh, was presented first by Kuznetsov (1968). It was applied by Fortin and Teman (1971) and by Ladevèze and Peyret (1974) using the projection method which, according to Peyret and Taylor (1983), seems to be more efficient in the MAC mesh, what may explain its rare use.

However, a systematic comparison between the semi-staggered, staggered, cell-center collocated and vertex collocated meshes in the lid driven hydrodynamic cavity test problem, with explicit time integration, Figueiredo and Moraes de Oliveira (2009a,b) indicated that the stability and the accuracy of the semi-staggered mesh is comparable to the best ones, the staggered and the cell-center collocated meshes.

Analogously to the collocated meshes, the collocated velocity components of the semi-staggered mesh simplify the computation of the momentum fluxes, since the influence coefficients are the same for both momentum components. On the other side, the semi-staggered mesh shares with the staggered mesh the simple closure of the pressure equations, by maintaining the boundary velocities when taking the numerical divergence of the local momentum equation. Also, the semi-staggered mesh, as well as the vertex collocated mesh, allows the use of entirely regular spacing of both velocity components.

As both collocated meshes, the semi-staggered mesh produces oscillating pressure fields. A momentum interpolation procedure analogous to the Rhie and Chow is possible, that smoothes the pressure field at the price of loosing the strict observance to the numerical continuity equation. Alternatively, such procedure can also be used only as post processing, without perturbing the solenoidal velocity field, in order to smooth the pressure field.

2.2 UNIFAES

The present work employs the Unified Finite Approach Exponential-type Scheme, UNIFAES, to compute the advective and viscous terms of the momentum equations. This scheme belongs to a class of schemes whose interpolating functions are obtained as exact solutions of a one dimensional linear equation, which somehow approximates the equation of interest. Let us consider the two-dimensional momentum transport equation in non-dimensional form, in terms of a dummy variable ϕ :

$$\frac{\partial \phi}{\partial t} + Re\frac{\partial (u\phi)}{\partial x} + Re\frac{\partial (v\phi)}{\partial y} - \frac{\partial^2 \phi}{\partial x^2} - \frac{\partial^2 \phi}{\partial y^2} = S \tag{1}$$

In general terms, the exponential-type schemes use as interpolating curve the exact solution of the one-dimensional equation:

$$Reu\frac{d\phi}{dx} - \frac{d^2\phi}{dx^2} = K \tag{2}$$

This linear equation approximates the transport Eq.(1) around each boundary cell, by assuming the velocity to be locally constant, as well as the cross advective and diffusive fluxes, transient and source terms of the partial Eq.(1), which are represented by the non-homogeneous term . Such schemes could be expressively called Locally Analytic for their conception. Indeed such name was adopted by one particular scheme of the class (LOADS). Alternatively they may be called Exponential-type Schemes, since the exponential function appears in their interpolating curves and in their influence coefficients.

The class of Exponential-type schemes founded upon one-dimensional generating equations started with the Allen and Southwellńs finite differencing exponential scheme (Allen and Southwell, 1955). The methodology due to Allen was rediscovered by other authors using finite dif-

ferencing, finite element and, particularly, finite volume methods. A brief review of such work is presented by Figueiredo and Moraes de Oliveira (2009b), the present paper concentrates on the finite volume schemes.

The first exponential schemes proposed in the finite volume approach (Spalding, 1972; Raithby and Torrance, 1970) were based on a homogeneous generating equation associated to Eq.2, so loosing much of the similarity with the original equation. At the price of greater algorithmic complexity and bigger computational time spending, the non-homogeneous generating equation was recovered by the finite volume schemes Locally Analytic Differencing Scheme, LOADS, (Wong and Raithby, 1979), Flux-Spline Scheme, (Varejão, 1979; Karki et al., 1989) and, at last, the Unified Finite Approaches Exponential-type Scheme, UNIFAES (Figueiredo, 1997).

All those schemes are naturally upwinded (Calhoon Jr. and Roach, 1997), in the sense that the influence coefficients of the upwind neighbor nodes become increasingly dominant as the cell Reynolds number increases, although the computational molecule remains symmetric except at the limit for infinite Reynolds numbers.

All exponential-type schemes are asymptotically second order, but at high Reynolds numbers the Allen and Southwell scheme and the simple Exponential Scheme approach the first order upwind scheme, justifying some criticisms to their slow spatial convergence (Leonard and Drummond, 1975). However, the exponential-type finite volume schemes based on non-homogeneous generating equations, namely LOADS, Flux-Spline and UNIFAES, are effectively second order at any Reynolds number, being not liable to Leonard and Drummondńs criticism.

The greater computational time spending of the exponential function compared to polynomial discretizations is another source of criticism which, on one hand, motivated the development of approximations such as the Power-Law Scheme (Patankar, 1980) and Padé approximants (Axelsson and Gustafsson, 1979). The Power-Law approximation was also employed in UNIFAES (Figueiredo and Llagostera, 1999; Llagostera and Figueiredo, 2000b,a).

UNIFAES was initially submitted to a series of tests representing eigenfunctions of the linear advective-diffusive transport equation on a uniform flow field (Figueiredo, 1997). It showed stability even at Peclet numbers as high as 109 and very good accuracy in all eigenfunctions, generally overcoming the central differencing, the simple exponential and LOADS. It presented no significant effects of the flow-to-grid angle. The distance of UNIFAES to the other schemes increased for crescent Peclet numbers. On the other side, all schemes tended to produce equally higher errors as the function eigenvalue increased.

Then UNIFAES was submitted to the Smith and Hutton test problem, concerning the transport of a scalar in a prescribed curved velocity field, for Peclet numbers up to 106 (Figueiredo and Llagostera, 1999). Again it presented very good performance, generally overcoming the other schemes, except the central differencing in a range of Peclet numbers where this scheme showed extremely high accuracy and unusual stability up to Peclet number 10,000. It also presented very good performance in simple one-dimensional tests concerning grid irregularity (Llagostera and Figueiredo, 2000b,a).

Then, the Power-Law form of UNIFAES was applied to the thermal transport equation on a buoyant Darcian porous flows involving natural and mixed convection in different geometries (Figueiredo and Llagostera, 1999; Llagostera and Figueiredo, 2000b,a). Some comparisons with the simple Power Law scheme also showed the crescent superiority of UNIFAES as the Rayleigh number increased.

Finally, the comparison of UNIFAES with central differencing and the simple exponential

scheme was extended to the case of the incompressible Navier-Stokes equations in primitive variables, considering all fundamental mesh structures, employing the classic test problems of the 2D lid-driven cavity flow in the standard form (with uniform lid velocity) and in the regularized form (that removes the singularity at the lid corners) (Figueiredo and Moraes de Oliveira, 2009b,a). The reader is also referred to such papers for details on the governing equations, on the method of solution and on the methodology of Richardson extrapolation.

A simplified presentation of the Finite Volume Exponential-type Schemes for discretization of the advective and viscous transport of momentum, particularly UNIFAES, is given here. Algebraic details are found in (Figueiredo, 1997; Figueiredo and Llagostera, 1999).

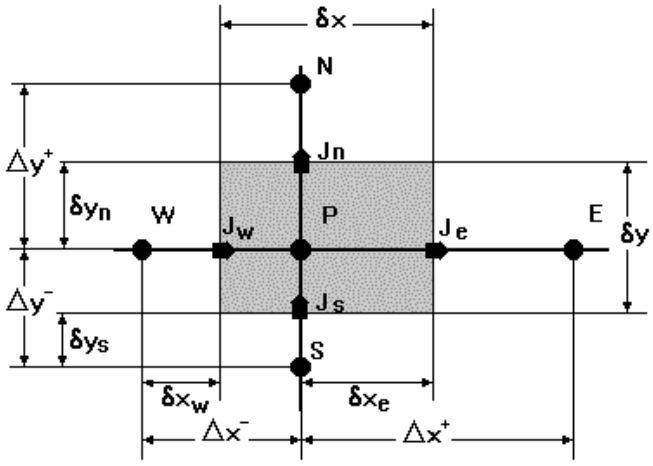

Figure 2: Rectangular control volume with the compass notation

Figure 2 reproduces a rectangular control volume with the usual Finite Volume compass notation, showing the advective-viscous fluxes located at the intersection of its parallel coordinate and its orthogonal cell face. The combined net advective and viscous flux

$$A_\phi = Re\frac{\partial(u\phi)}{\partial x} + Re\frac{\partial(v\phi)}{\partial y} - \frac{\partial^2\phi}{\partial x^2} - \frac{\partial^2\phi}{\partial y^2} \tag{3}$$

is integrated on the cell volume v and is transformed, through to the divergence theorem, into the integral of the advective-viscous flux through the cell surface. For all control volume locally analytic schemes, the integrated net flux is given by:

$$\int_v \int A_\phi dv \cong a_E(\phi_E - \phi_P) + a_W(\phi_W - \phi_P) + a_N(\phi_N - \phi_P) + a_S(\phi_S - \phi_P) - \psi \tag{4}$$

where

$$a_{E/W} = \pi(\pm p_{e/w})\delta y/\delta x^{\pm} \tag{5}$$

$$a_{N/S} = \pi(\pm p_{n/s})\delta x/\delta y^{\pm} \tag{6}$$

$$p_{e/w} = Re\ u_{e/w}\ \Delta x^{\pm} \tag{7}$$

$$p_{n/s} = Re\ v_{n/s}\ \Delta y^{\pm} \tag{8}$$

$$\pi(p) = \frac{p}{exp(p) - 1} \tag{9}$$

$$\psi = [K_e\ \Delta x^{+}\chi(p_e) - K_w\ \Delta x^{-}\chi(p_w)]\delta y + [K_n\ \Delta y^{+}\chi(p_n) - K_s\ \Delta y^{-}\chi(p_s)]\delta x \tag{10}$$

$$\chi(p) = \frac{\pi(p) - 1}{p} + R \tag{11}$$

$$R = \frac{\delta x_{e/w}}{\Delta x^{\pm}} \ \ or \ \ R = \frac{\delta y_{n/s}}{\Delta y^{\pm}} \tag{12}$$

In Eqs.(5) to (8) and (12), indexes e and n correspond to sign +, and indexes w and s to sign -.

The simple exponential scheme (Spalding, 1972; Raithby and Torrance, 1970; Patankar, 1980) is recovered by assuming null K., so dismissing Eqs. (10) to (12). The complete equations are relevant for LOADS and UNIFAES, and, with minor changes, for the Flux-Spline scheme.

In UNIFAES, the information about K is provided by the finite differencing approach that led to the Allen and Southwell scheme (Allen and Southwell, 1955). The Allen and Southwell exponential scheme computed the analogue of the net advective and diffusive fluxes in non conservative form by employing the generating equation analogous to Eq. 2, but centered on node P. Generalizing the Allen and Southwell scheme for irregularly spaced grids one obtains:

$$K_p = (\phi_p - \phi_E)\Pi^{+} + (\phi_P - \phi_W)\Pi^{-} \tag{13}$$

where $\Pi^{\pm}$ was put by Llagostera and Figueiredo (2000a,b) in a form adequate for using any approximation of the function :

$$\Pi^{\pm} = \frac{Re\ u_p\ \pi(\pm p_u^{\pm})}{\Delta x^{\pm}[\pi(-p_u^{-}) - \pi(p_u^{+})]} \tag{14}$$

where

$$p_u^{\pm} = Re\ u_p\ \Delta x^{\pm} \tag{15}$$

In uniform grids, Eq. (14) reduces to the original Allen and Southwell scheme:

$$\Pi^{\pm} = \frac{\pi(\pm p_u^{\pm})}{\Delta x^2} \tag{16}$$

In UNIFAES, the source term $K_e^{i,j}$, for instance, is found by linear interpolation of the generalized Allen and Southwell estimates of K_p on the nodes (i, j) and $(i + 1, j)$. Although the Allen and Southwell scheme is non-conservative, its use in UNIFAES maintains numerical conservation because $K_e^{i,j} = K_w^{i+1,j}$, so that $J_e^{i,j} = J_w^{i+1,j}$. The 2D computational molecule around node (i, j) involves the immediate neighbors $(i \pm 1, j)$ and $(i, j \pm 1)$ and also the remote nodes $(i \pm 2, j)$ and $(i, j \pm 2)$. At the cell boundaries neighbor to the domain frontiers, is linearly extrapolated from the closest internal nodes, dismissing the remote node outside the domain.

2.3 Numerical setup

The domain of study was the same of Lee and Mateescu (1998). The expansion ratio ER=(S+h)/h tested was 2.0. The characteristic dimension D is the neck hydraulic diameter, $D = 2h$. The definition of Reynolds is the same of Armaly et al. (1983) and is calculated as:

$$Re = \frac{VD}{\nu} \tag{17}$$

where V is the mean velocity at the entrance and ν is the kinetic viscosity.

The dimensionless values used were h=0.5, S=0.5, L=10 for 100$\leq$Re$\leq$600, L=15 for Re=800 and Re=1000 and L=25 for Re=1200. For the cases with entrance channel c=5.0; otherwise, c=0.

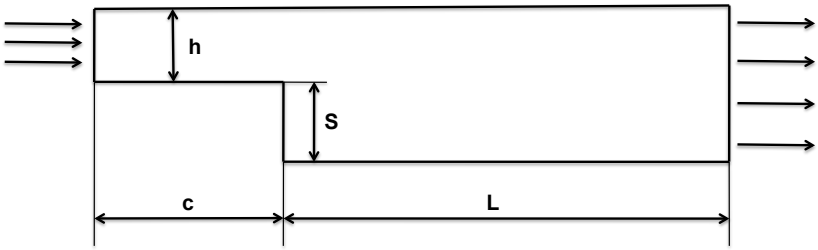

Figure 3: Sketch of the step geometry defining various geometrical parameters.

A parabolic profile of a developed flow was imposed in the inlet region. thertefore, the mean velocity at the inlet is $2/3$ of the maximum inlet velocity. The walls are non-slip. Homogeneous Neumann boundary condition were assumed for the velocity components at the domain outlet.

Three different sets of mesh sizes Δx and Δy were simulated for each Reynolds number. The less refined one had Δx=0.25 and Δy=0.025, the intermediary one had Δx=0.125 and Δy=0.0125 and the most refined case Δx=0.0833 and Δy=0.00833.

Schematic location of the two recirculation zones that can be present in the flow and the three main points of detachment or reattachment can be seen at Fig. 4.

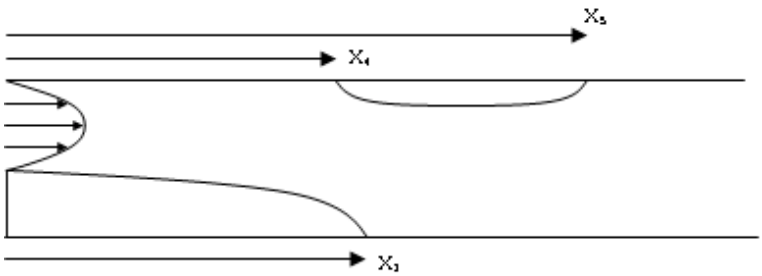

Figure 4: Location of detachment and reattachment points

3 RESULTS

There is little information about the importance of entrance channel in study of backward-facing step flow, Kaiktsis et al. (1991) says that "the profile imposed at different upstream location results in negligible differences in the flow field, unless the Reynolds number is very

low ($Re \leq 200$); for $Re \leq 200$, the value of X_1 is overpredicted by almost 10% if the inflow boundary is taken exactly at the step expansion". In face of this affirmations a study a X_1 value studied was conducted for two differents Reynolds values, Re=100 and Re=600, keeping always the same mesh size Δx=0.25 and Δy=0.025 for the different channels lengths. The results of this study can be seen at Table 1.

Channel Length	X_1, Re=100	X_1, Re=600
0	3.253	10.601
1	3.144	10.300
2	3.142	10.306
3	3.142	10.305
4	3.142	10.305
5	3.142	10.305
6	3.142	10.305

Table 1: X_1 values for different entrance length channel

Table 1 shows that the inlet channel plays some role in the X_1 results. The computations without the channel presented about 3% larger reattachments lengths for both Reynolds numbers, in disagreement with Kaiktsis et al. (1991).

These results were used to defined a channel length of 5 as standard in the next simulations, whose main purpose is to compare the experimental data from Lee and Mateescu (1998) with the simulations with and without the channel.

Figure 5 and 6 show the profiles of the u velocity exactly at the step expansion for Re=100 and Re=600 respectively, for the cases without entrance channel and with entrance channel of length 5.

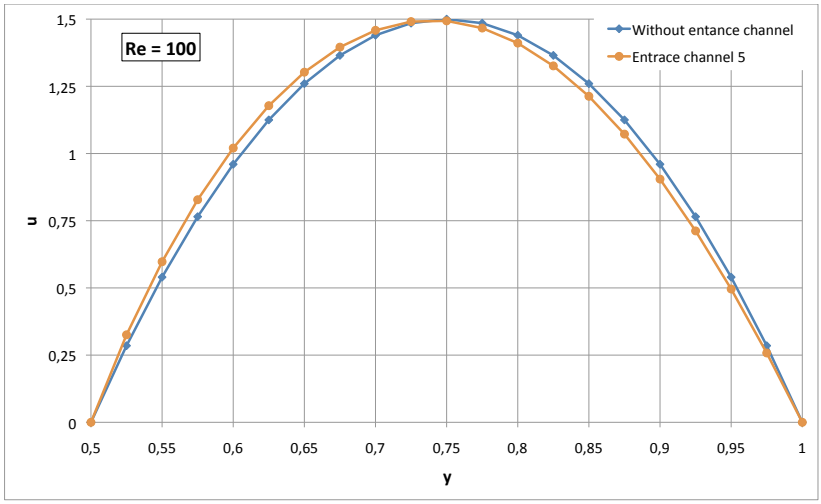

Figure 5: Re=100, Profiles of u velocity in the step expansion for simulation without entrance channel and with a length entrance channel of 5

The main difference between the two cases that can be seen in fig. 5 is the presence of a non-symmetric, decentralized flow profile at the step plane for the case with entrance channel, instead of the assumed symmetric profile for the case without entrance channel. Slightly greater values of u velocity are found near the expansion step (y=0.5) and smaller values near the channel wall (y=1.0) if compared with the imposed symmetric profile.

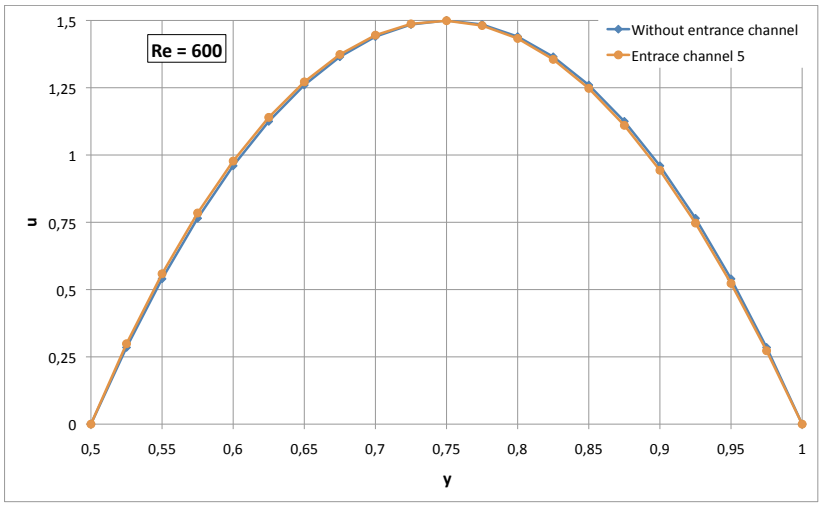

Figure 6: Re=600, Profiles of u velocity in the step expansion for simulation without entrance channel and with a length entrance channel of 5

The same non-symmetric, decentralized flow profile at the step plane for the case with entrance channel is found at fig. 6 where can be found the results for Re=600. Again the biggest difference between the cases is found around y=0.5 but the differences between the cases with and without entrance channel is much smaller than for the lower Reynolds number.

Figure 7 shows the variation of the location of the reattachment point at the lower wall x_1 as function of the Reynolds numbers. Comparing the two present numerical data, the first important difference is that the size of first bubble is smaller when the entrance channel is used, for whole the Reynolds range studied. This is due the decentralized flow profile at the step plane, where higher velocities are founded near y=0.5. Numerical simulation with the entrance channel has better agreement with the experimental data until Re=600, when both numerical 2-D simulation results start to have bigger differences with the experimental results.

Variation of the location of detachment and reattachment points at the upper wall x_4 and x_5 as function of the Reynolds numbers are plotted at Fig. 8. Experimental data from Lee and Mateescu (1998) are compared with the present numerical simulations with and without entrance channel. The second bubble is bigger, starting and finishing upstream in the case where the entrance channel is used compared with the case without entrance channel. This is due to the influence of the first bubble attached to the lower wall that also finished upstream for the case where the entrance channel is present, forcing the beginning of the second bubble attached in the upper wall. Another observation during the simulations, not show here, is that this second recirculation starts to be presented at a lower Reynolds number with the entrance

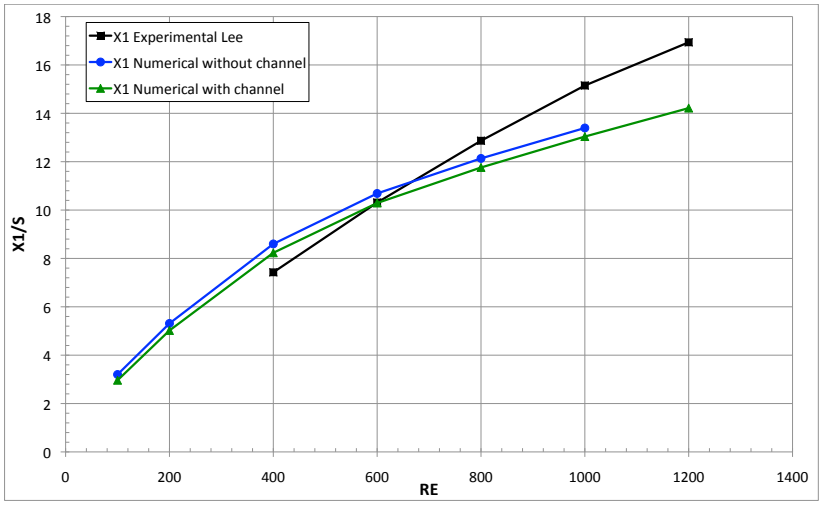

Figure 7: Variation of location of reattachment points at lower wall x_1 with Reynolds numbers. Experimental data from Lee and Mateescu (1998), presented numerical data without entrance channel and presented numerical data with entrance channel of length 5

channel.

Experimental and numerical data have a good agreement until Re=800, when x_4 values of experimental data stabilize and x_5 increase quickly, resulting in a smaller recirculation zone when compared with the simulation. Despite this facts, numerical results from the simulation with the entrance channel have better agreement with the experimental data until Re=600.

4 CONCLUSIONS

The influence of the entrance channel in the numerical simulation of the classic two-dimensional backward-facing step flow was studied. Location of detachment and reattachment and velocity profile as function of Reynolds number were obtained and compared with experimental data from Lee and Mateescu (1998).

Results showed a small but not ignorable influence of the entrance channel in the location of the detachment and reattachment points and in the size of the recirculation zones. Better agreement with experimental data was obtained for Re $\leq$ 600 when the inlet channel is employed. A non-symmetric, decentralized flow profile at the step plane was found for the cases with entrance channel.

The combination of the semi-staggered mesh with the UNIFAES discretization scheme showed good stability and precision in all the cases presented here.

It is clear that the introduction of the inlet slot, by itself, is not sufficient to approach the experimental results for Reynolds numbers above, say, 700.

The significant departure of both numerical solutions with respect to the experimental results must be attributed to the three-dimensionality of the experimental set, in two aspects. First, because of the side effects neglected by the 2D model. Second, because of the physical instabilities that start to appear around Re$\cong$700. Consequently, further theoretical approach to the experimental results are expected after obtaining 3D numerical results.

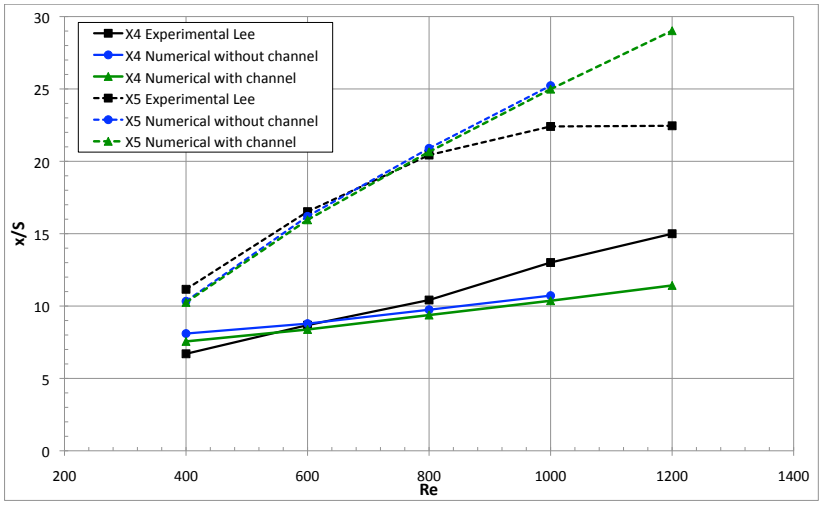

Figure 8: Variation of location of detachment and reattachment points at upper wall x_4 and x_5 with Reynolds numbers. Experimental data from Lee and Mateescu (1998), presented numerical data without entrance channel and presented numerical data with entrance channel of length 5

5 ACKNOWLEDGMENTS

The authors acknowledge the financial support from research funding agencies FAPESP (Fundação de Amparo à Pesquisa do Estado de São Paulo) and CNPQ(Conselho Nacional de Desenvolvimento Científico e Tecnológico).

REFERENCES

Allen D.N.d.G. and Southwell R. Relaxation methods applied to determine the motion, in two dimensions, of a viscous flow past a fixed cylinder. *Quart. J. Mech. and Applied Math.*, 8:129–145, 1955.

Armaly B., Durst F., Pereira J., and Schounung B. Experimental and theoretical investigation of backward-facing step flow. *JOURNAL OF FLUID MECHANICS*, 127(FEB):473–496, 1983.

Axelsson O. and Gustafsson I. A modified upwind scheme for convective transport equations and the use of a conjugate gradient method for the solution of non-symmetric systems of equations. *J. Inst. Maths. Applics.*, 23:321–337, 1979.

Calhoon Jr. W.H. and Roach R.L. A naturally upwinded conservative procedure for the incompressible navier-stokes equations on non-staggered grids. *Computers and Fluids*, 26(5):525–545, 1997.

Figueiredo J.R. A unified finite-volume finite-differencing exponential-type convective-diffusive fluid transport equations. *J. Braz. Society Mech. Sci.*, 3:371–391, 1997.

Figueiredo J.R. and Llagostera J. Comparative study of the unified finite approaches exponential-type scheme (unifaes) and its application to natural convection in a porous cavity. *Numerical Heat Transfer, B*, 35:347–367, 1999.

Figueiredo J.R. and Moraes de Oliveira K.P. Comparative Study of the Accuracy of the Fundamental Mesh Structures for the Numerical Solution of Incompressible Navier-Stokes Equa-

tions in the Two-Dimensional Cavity Problem. *NUMERICAL HEAT TRANSFER PART B-FUNDAMENTALS*, 55(5):406–434, 2009a.

Figueiredo J.R. and Moraes de Oliveira K.P. Comparative Study of UNIFAES and other Finite-Volume Schemes for the Discretization of Advective and Viscous Fluxes in Incompressible Navier-Stokes Equations, Using Various Mesh Structures. *NUMERICAL HEAT TRANSFER PART B-FUNDAMENTALS*, 55(5):379–405, 2009b.

Fortin M.; Peyret R. and Teman R. Résolution numérique des equations de navier-stokes pour un fluide incompressible. *J. Mécanique*, 3:357–390, 1971.

Kaiktsis L., Karniadakis G.E., and Orszag S.A. Onset of three-dimensionality, equilibria, and early transition in flow over a backward-facing step. *Journal of Fluid Mechanics*, 231(-1):501–528, 1991.

Karki K.C., Patankar S.V., and Mongia M.C. Solution of three-dimensional flow problem using a flux-spline method. *AIAA*, 1989.

Kuznetsov B.G. Numerical methods for solving some problems of fluid flow. *Fluid Dynamics Transactions*, 4:85–89, 1968.

Ladevèze J. and Peyret R. Calcul numérique d'une solution avec singularitè des equations de navier-stokes: Écoulement dans un canal avec variation brusque de section. *J. Mécanique*, 13(3):367–396, 1974.

Lee T. and Mateescu D. Experimental and numerical investigation of 2-D backward-facing step flow. *JOURNAL OF FLUIDS AND STRUCTURES*, 12(6):703–716, 1998.

Leonard B.P. and Drummond J.E. Why you should not use 'hybrid', 'power-law' or related exponential schemes for convective modelling - there are much better alternatives. *Int. J. Numerical Methods in Fluids*, 20:421–442, 1975.

Llagostera J. and Figueiredo J.R. Application of the unifaes discretization scheme to mixed convection in a porous layer with a cavity, using the darcy model. *J. Porous Media*, 3(2):139–154, 2000a.

Llagostera J. and Figueiredo J.R. Numerical study on mixed convection in a horizontal flow past a square porous cavity using unifaes scheme. *J. Braz. Soc. Mech. Sci.*, 4:583–597, 2000b.

Patankar S.V. *Numerical Heat Transfer and Fluid Flow*. McGraw-Hill, 1980.

Peyret R. and Taylor T.D. *Computational Methods for Fluid Flow*. Springer-Verlag, 1983.

Raithby G.D. and Torrance K.E. Upstream-weighted differencing schemes and their application to elliptic problems involving fluid flow. *Computers and Fluids*, 2:191–206, 1970.

Spalding D.B. A novel finite difference formulation for differential expressions involving both first and second derivatives. *Int. J. Numer. Meth. Eng.*, 4:551–559, 1972.

Varejão L.M.C. *Flux-Spline Method for Heat and Momentum Transfer*. Ph.D. thesis, University of Minnesota, 1979.

Wong H.H. and Raithby G.D. Improved finite-difference methods based on a critical evaluation of the approximation errors. *Numerical Heat Transfer*, 2:139–163, 1979.